

Pilot-based detection for DVB-T passive coherent location radars

 ISSN 1751-8784
 Received on 9th June 2019
 Revised 24th October 2019
 Accepted on 18th February 2020
 E-First on 14th April 2020
 doi: 10.1049/iet-rsn.2019.0268
 www.ietdl.org

 Osama Mahfoudia¹ ✉, François Horlin², Xavier Neyt³
¹Ecole Militaire Polytechnique, BP 17, Bordj el Bahri, Algiers, Algeria

²Université libre de Bruxelles, Avenue Franklin Roosevelt 50, 1050 Brussels, Belgium

³Royal Military Academy, Avenue de la Renaissance 30, 1000 Brussels, Belgium

✉ E-mail: osama.mahfoudia@gmail.com

Abstract: This study investigates the feasibility of pilot-based detection for passive coherent location (PCL) radars exploiting digital video broadcasting-terrestrial (DVB-T) signals. The DVB-T signal is formed by two parts: a data signal and a pilot signal. The parameters of the pilot signal are known thanks to the DVB-T standards that permit the generation (at the receiver) of the pilot signal. The pilot recovery technique, based on the known DVB-T standard, is utilised in DVB-T based PCL systems to reduce the number of the reception channels by considering a locally generated pilot signal as a reference signal. Consequently, no reference channel is required, which reduces the cost and the complexity of the resulting PCL system. In this work, the authors propose a signal processing method to achieve this goal. They consider theoretical analysis, simulations and real-data results to validate the feasibility of such a system.

1 Introduction

The first radar systems were bistatic, where the transmitter and the receiver are separated by a considerable distance [1]. Then, with advances in technology, especially the creation of the duplexer in 1936, monostatic radars have dominated the radar research and design fields. However, the interest on bistatic radars has been reinforced due to the technology advances such as high dynamic range analogue-to-digital converters and the computer core technology [2], the resulting systems are called passive radars. The essential advantages of passive radars are the spatial dislocation between the transmitter and the receiver, and the use of the pre-existing transmitter infrastructure [3].

Passive radar systems can exploit another radar or commercial transmitters. The passive radar is called a hitchhiker if another radar is exploited [1]. Otherwise, we refer as passive coherent location (PCL) radars to the radars exploiting commercial transmitters [4, 5]. In PCL radar systems, the exploited transmitters are known as illuminators of opportunity (IO). With the existence of several possibilities of IOs, the PCL concept is gaining a growing interest. In the literature, we can find a large variety of IOs exploited in PCL systems such as frequency modulation radio [6, 7], global system for mobile communications [8, 9], digital audio broadcasting [10, 11] and digital video broadcasting-terrestrial (DVB-T) [12, 13].

The selection of an illumination source is performed by considering three key parameters, which we note in the following. Firstly, the transmitted power of the exploited illuminator of opportunity will define the detection coverage of the PCL system [4]. Secondly, the bandwidth of the exploited signal will precise the range resolution [5]. Thirdly, the ambiguity function (AF) of the exploited signal; the AF is used to evaluate the suitability of a waveform for radar applications. In fact, the exploited signals are not designed for radar applications, which leads in most cases to ambiguities in range and in Doppler, and thus results in false alarms and ghost targets [5]. Analogue waveforms are characterised by an AF full of ambiguities in range and Doppler, which will disturb the PCL applications. However, digital waveforms have a thumbtack shape AF, which is suitable for PCL systems [8].

A PCL system requires two reception channels: a reference channel and a surveillance channel [13]. The antenna of the

reference channel is pointed to the direction of the illuminator of opportunity to acquire the direct-path signal. For the surveillance channel, the antenna is steered towards the surveillance area to collect the possible target echoes. In addition to the echoes of interest, the surveillance signal includes a strong direct-path signal and returns from static scatterers [13]; these unwanted contributions are called the static clutter. In practice, the power of the static clutter signal is several orders of magnitude larger than the target return which reduces the detector dynamic range and buries low-return targets [5]. In the literature, many methods have been proposed for the static clutter suppression [14–16].

Bistatic PCL systems can determine the bistatic range by measuring the difference in time of arrival between the reference signal and the target echo [1]. In addition to the bistatic range, the Doppler shift of the target echo can be retrieved. It follows that the reference signal quality is of a great importance for the detection. A reference signal with low signal-to-noise ratio (SNR) degrades the detection probability [17–20]. This scenario can be noticed if the distance separating the receiver site and the exploited IO is considerable.

DVB-T signals are widely used for PCL systems [12, 13]. With a transmitted power in the order of 10 kW, they can ensure medium range coverage applications. Also, their bandwidth is 7.61 MHz, which allows a range resolution of ~30 m. In addition, their AF has a thumbtack shape, which is suitable for PCL applications. Other advantages of the DVB-T signals are related to the signal structure. In fact, the DVB-T signal structure is known, which allows the reconstruction of the reference signal to enhance its quality. The signal reconstruction is performed by demodulating the received signal and recoding the retrieved symbols to retrieve a noise-free version of the transmitted signal [12, 13, 21, 22]. This approach is efficient if the initial SNR guarantees a low-error demodulation of the received signal. For low SNR values, the performance of the signal reconstruction is limited [23, 24].

The DVB-T signal can be modelled as the sum of two components: a data signal which depends on the content to broadcast, and a pilot signal which is employed for synchronisation and channel estimation purposes [25, 26]. The pilot signal can be generated at the receiver since it is fully known [27], which results in the possibility of using it for detection in the DVB-T based PCL systems as a replacement of the reference signal. The resulting system includes a single receiver, which reduces the system cost.

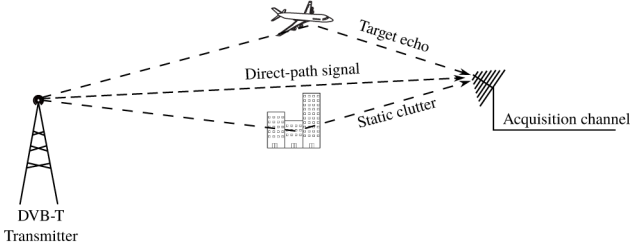


Fig. 1 Considered configuration and signal model

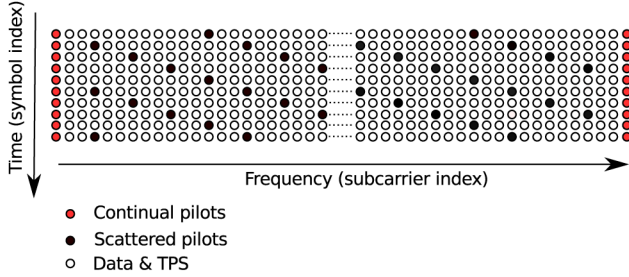


Fig. 2 DVB-T signal structure

Table 1 Main parameters of the DVB-T signal

Parameter	2K mode	8K mode
number of subcarriers K	1705	6817
number of data subcarriers K_d	1512	6048
number of pilot subcarriers K_p	176	701
number of TPS subcarriers K_{TPS}	17	68
useful symbol duration T_U	224 μ s	896 μ s
subcarrier spacing Δf	4464 Hz	1116 Hz
signal bandwidth B	7.61 MHz	7.61 MHz

In [28], a first approach has been made to exploit this possibility, where the pilot signal is employed to replace the reference signal in noisy scenarios. The simulation results showed that the use of a pilot signal provides better results than using a noisy reference signal. However, for high SNR values, using a pilot signal provides lower performances compared to the full signal. Moreover, the signal synchronisation and the static clutter suppression step were not considered. In this work, we propose an improved method for detection in DVB-T based PCL radars employing pilot signal, which includes a static clutter suppression stage in the spectral domain through the propagation channel estimation [16, 29]. In addition, the synchronisation stage is analysed and its performance are discussed. The performances of the proposed method are verified by simulation results and validates through the application on real data.

The paper is organised as follows. Section 2 describes the model of the received and DVB-T signals. In Section 3, we present the detection strategy which includes the stages of signal synchronisation, static clutter suppression and target detection. The results and discussions are presented in Section 4. Finally, Section 5 summarises the major retrievals of this work.

2 Signal model

In this section, we present the considered model for the received signal and we define the DVB-T signal structure. In this work, we consider a bistatic PCL radar based on DVB-T IO. We note $s(n)$ the transmitted signal with a variance of σ_s^2 . Fig. 1 presents the configuration of the considered system; it shows the different components of the received signal $x(n)$. This signal can be defined by considering the following binary hypotheses:

$$\begin{cases} H_0: x(n) = \sum_{l=0}^{L-1} h_l s(n-l) + v(n), \\ H_1: x(n) = \sum_{l=0}^{L-1} h_l s(n-l) + \alpha s(n-\kappa) e^{j2\pi f_d n} + v(n). \end{cases} \quad (1)$$

Under the null hypothesis (H_0), the received signal includes direct-path and multipath components in addition to a thermal noise. In this model, we consider L multipath components (including the direct-path signal defined by $h_0 s(n)$) with complex weights h_l ; this contribution is called static clutter. We note $v(n)$ the thermal noise of a variance σ_v^2 and with a centred complex Gaussian distribution. Under the alternative hypothesis (H_1), the received signal involves a target echo in addition to static clutter and thermal noise. The target echo is an attenuated copy of the transmitted signal time-delayed by τ and frequency-shifted by f_d . The attenuation α includes all the effects undergone by the target echo (antenna gain, propagation losses and target reflectivity). We define three important parameters related to the received signal: the direct-path-to-noise ratio (DNR), the clutter-to-noise ratio (CNR) and the SNR of the target return, which are given by the following expressions [13, 20]:

$$\text{DNR} = |h_0|^2 \sigma_s^2 / \sigma_v^2, \quad (2)$$

$$\text{CNR} = \sum_{l=0}^{L-1} |h_l|^2 \sigma_s^2 / \sigma_v^2, \quad (3)$$

and

$$\text{SNR} = |\alpha|^2 \sigma_s^2 / \sigma_v^2. \quad (4)$$

The DVB-T signal is generated following a multicarrier modulation known as orthogonal frequency division multiplexing (OFDM). The generated signal is structured into symbols; each symbol includes a useful part and a cyclic prefix. The useful part is formed by a large number of orthogonal and equally spaced subcarriers [27]. In time domain, the signal model for one DVB-T symbol is expressed as follows:

$$s(n) = \sum_{k=0}^{K-1} c(k) e^{j2\pi f_k n}, \quad (5)$$

where K subcarriers are employed and each one is of a frequency f_k and modulated by a quadrature amplitude modulation (QAM) symbol $c(k)$. The resulting DVB-T signal, $s(n)$, follows a complex Gaussian distribution with zero mean and variance σ_s^2 , i.e. $s(n) \sim \mathcal{CN}(0, \sigma_s^2)$ [30, 31].

Fig. 2 shows the structure of the DVB-T signal in the frequency domain. Three types of subcarriers constitute the DVB-T symbols: data subcarriers, transmission parameter signalling (TPS) subcarriers, and pilot subcarriers. Data subcarriers transport the useful data and TPS subcarriers convey the broadcasting parameters. The pilot subcarriers are used for the synchronisation of the received signal and for the propagation channel estimation. It follows that they are transmitted at known frequencies and with known amplitudes [27].

Table 1 summarises the main parameters of the DVB-T signal for both 2K and 8K modes, such as the number of subcarriers for each DVB-T symbol and the number of each carrier variant (data, TPS and pilot) in one symbol.

If we neglect the contribution of the TPS subcarriers, the time-domain DVB-T signal can be considered as the sum of two components a data signal, $d(n)$, and a pilot signal, $p(n)$. This can be expressed as follows:

$$s(n) = d(n) + p(n). \quad (6)$$

The pilot subcarrier amplitudes are obtained through a pseudo-random binary sequence [27]. By invoking the central limit theorem, we can consider that the time-domain pilot signal $p(n)$ follows a complex Gaussian distribution with zero mean and variance σ_p^2 , i.e. $p(n) \sim \mathcal{CN}(0, \sigma_p^2)$. Similarly, the data subcarriers are loaded by QAM symbols obtained from randomised binary data. This allows to assume that the time-domain data signal $d(n)$

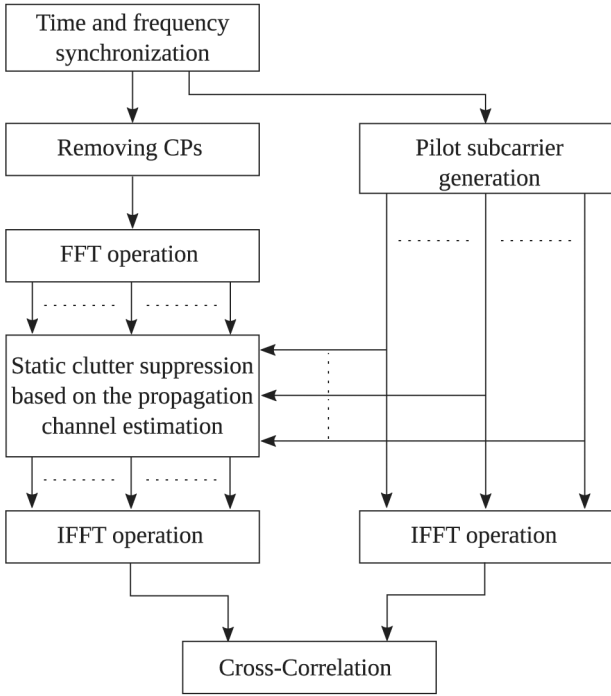


Fig. 3 Proposed detection strategy

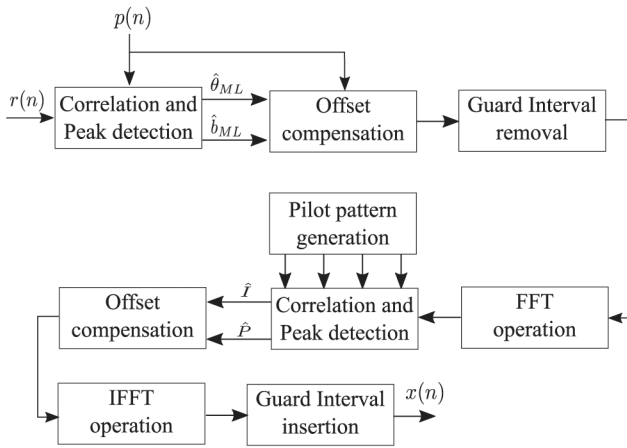


Fig. 4 Scheme of the received signal synchronisation

follows a complex Gaussian distribution with zero mean and variance σ_d^2 , i.e. $d(n) \sim \mathcal{C}\mathcal{N}(0, \sigma_d^2)$. In addition, the data signal $d(n)$ and the pilot signal $p(n)$ are statistically independent, which leads to the following result:

$$\sigma_s^2 = \sigma_d^2 + \sigma_p^2. \quad (7)$$

We can define the ratio between the data signal power and that of the pilot signal as follows:

$$\rho = \sigma_d^2 / \sigma_p^2. \quad (8)$$

The ratio ρ can be calculated through the parameters in Table 1. It can be found that $\rho \simeq 4.9$ for both 2K and 8K transmission modes.

3 Detection strategy

The present section details the proposed signal processing strategy. It performs the passive detection employing a locally generated pilot signal for DVB-T based PCL systems. Fig. 3 presents this strategy. Three main stages can be distinguished: the synchronisation of the received signal, the suppression of the static clutter and the target detection.

3.1 Signal synchronisation

As was mentioned in the previous section, the parameters of the pilot subcarriers are fully known, which allows the generation of a time-domain pilot signal at the receiver site. This signal is generated according to the DVB-T standard [27], which can be achieved by considering exclusively the amplitudes of pilot subcarriers (data and TPS subcarriers are set to zero). The pilot signal will be employed for detection as a replacement for the reference signal. To obtain a precise target localisation, an accurate synchronisation between the generated pilot signal and the received signal is required. The synchronisation stage compensates the possible time and frequency offsets between the two signals. In this work, the synchronisation is performed between the generated pilot signal and the direct-path component of the received signal $h_0 s(n)$.

Let us consider the following model for the received signal $r(n)$ with time and frequency offsets

$$r(n) = h_0 s(n - \theta) e^{j2\pi\phi n} + v_c(n), \quad (9)$$

where θ is the time offset, ϕ is the carrier frequency offset (CFO), and the term $v_c(n)$ includes the remaining terms from (1). The CFO ϕ is formed by two parts [32, 33]

$$\phi = \frac{b}{T_U} + \frac{I}{T_U}, \quad (10)$$

where $-0.5 \leq b \leq 0.5$, I is an integer, and T_U is the length of the DVB-T symbol useful part.

The signal synchronisation is a multi-stage operation, it includes two main stages: a pre-FFT stage and post-FFT stage [34, 35] as shown in Fig. 4. The pre-FFT stage exploits the guard interval redundancy to perform fine time synchronisation ($\hat{\theta}$) and fractional CFO estimation (\hat{b}). The aim of this stage is to determine the beginning of the DVB-T symbol to align it with the generated pilot signal. At this stage, the correlation between the received signal $r(n)$ and its delayed version is calculated and the resulting maximum value is determined [34]. The correlation is performed by considering many time delays m as follows:

$$\gamma(m) = \sum_{n=m}^{m+N_G-1} r(n)r^*(n+N_U), \quad (11)$$

where N_U is the number of samples of the DVB-T symbol useful part and N_G is the length of the guard interval. The maximum likelihood (ML) estimate of the time offset θ is given by [36]

$$\hat{\theta}_{ML} = \operatorname{argmax}_{\theta} (|\gamma(\theta)|). \quad (12)$$

The fractional CFO (the parameter b in (10)) can be estimated based on the retrieved value $\hat{\theta}_{ML}$ as follows:

$$\hat{b}_{ML} = \frac{-1}{2\pi} \angle \gamma(\hat{\theta}_{ML}). \quad (13)$$

Fig. 5 shows simulation results corresponding to (11) for a DVB-T signal with the 8K-mode. The magnitude peaks correspond to the beginning of the DVB-T symbols (the fractional time offset) and their phases give an ML estimation of the fractional CFO.

The retrieved parameters $\hat{\theta}_{ML}$ and \hat{b}_{ML} are exploited to align the two signals $p(n)$ and $r(n)$ and to compensate the fractional CFO. From the resulting signal, the guard interval is removed and the FFT is applied to retrieve the frequency domain version of the signal. The second stage of synchronisation retrieves the pattern of the pilot subcarriers for each DVB-T symbol (\hat{P}) and estimates the integer part of the CFO (\hat{I}). To do so, the correlation between the FFT result and the four patterns of the frequency domain pilot signal [27] is calculated and the maximum is determined. Based on

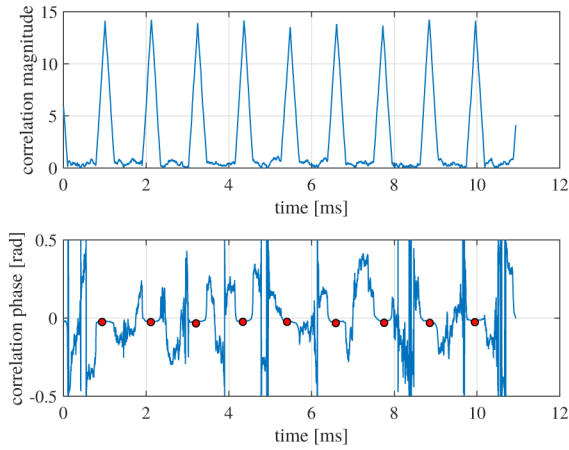


Fig. 5 ML estimation of fine time and fractional CFOs

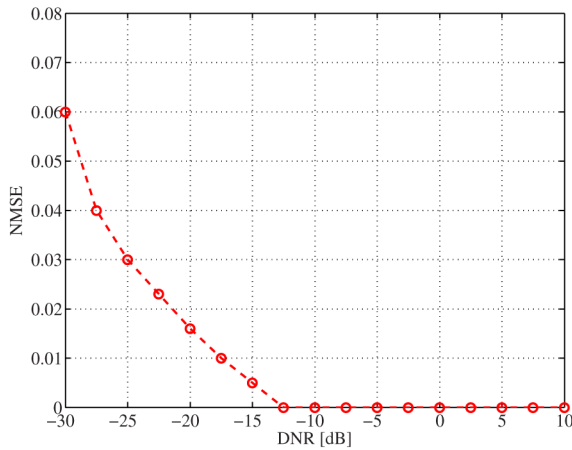


Fig. 6 NSME of the time-offset estimation as a function of the direct-path quality (DNR)

the maximum correlation value and its location, the two parameters \hat{P} and \hat{I} are estimated.

Consequently, the generated pilot signal can be perfectly synchronised with the received signal in time and frequency through the estimated parameters $\hat{\theta}_{ML}$, $\hat{\nu}_{ML}$, \hat{I} and \hat{P} .

To investigate the accuracy of the signal synchronisation ($\hat{\theta}_{ML}$), we propose to evaluate the normalised mean square error (NMSE) related to the time synchronisation. In Fig. 6, the NMSE of the time offset ML estimation is presented. The results show that it is possible to achieve an accurate time synchronisation, with an NMSE lower than 0.01, for scenarios with DNR values greater than -15 dB. Consequently, it is possible to obtain a precise target detection for these scenarios.

3.2 Static clutter suppression

As was stated earlier, the static clutter is formed by the direct signal from the exploited transmitter and the different multipaths caused by the stationary scatterers in the area. The presence of the static clutter reduces the detection dynamic range, which masks the weak target echoes. Therefore, the suppression of this undesirable contribution is required to enhance the target detection [37]. Several methods have been proposed for the static clutter suppression in PCL radars such as the adaptive filters [37] and the extensive cancellation algorithm (ECA) [14]. In addition, there are other methods dedicated for OFDM waveforms like the ECA by carrier (ECA-C) algorithm [15, 38]. The specificities of the OFDM signals are also exploited in the method proposed in [16, 29] which is based on the propagation channel estimation.

The method of the channel estimation for the static clutter suppression assumes an invariant propagation channel response during the considered experiment duration [16, 29]. It estimates the response of the propagation channel in the frequency domain by

exploiting the pilot subcarriers [39]. Then, this estimate is employed to generate an estimation of the static clutter which will be subtracted from the received signal. This method is characterised by a low complexity since no matrix inversion nor an adaptive processing are required. However, it requires the knowledge of the transmitted QAM data symbols to obtain an estimation of the static clutter signal.

In this work, we propose a modified version of channel estimation method for the static clutter suppression. In this approach, we reject the non-pilot subcarriers of the received signal since they will not participate in the integration gain. Then, the static clutter suppression is only performed over the pilot subcarriers. In the proposed method, we firstly synchronise the received signal in time and frequency as presented in the previous section. Then, the synchronised signal is divided into DVB-T symbols, the cyclic prefix (CP, or guard interval) is removed and an FFT is applied. The resulting signal is the frequency-domain representation of the received signal. For the k th subcarrier, the result can be expressed as follows:

$$X(k) = H(k)c(k) + X_t(k) + V(k), \quad \text{with } k = 1, \dots, K \quad (14)$$

where H is the propagation channel response, X_t is the target signal in the frequency domain and V is the FFT of the thermal noise v . Knowing the pilot subcarrier positions, we can select the components of X which correspond to the pilot subcarriers. We note X_p , H_p , c_p , $X_{t,p}$ and V_p the selected parts of the signal X . Thus, we can note

$$X_p(k) = H_p(k)c_p(k) + X_{t,p}(k) + V_p(k), \quad \text{with } k = 1, \dots, K_p \quad (15)$$

The least squares estimate of the propagation channel H_p is obtained by neglecting the target echo magnitude compared to the static clutter signal since $\text{CNR} \gg \text{SNR}$. An estimation of $H_p(k)$ can be obtained as follows:

$$\hat{H}_p(k) = X_p(k)/c_p(k) \quad \text{with } k = 1, \dots, K_p \quad (16)$$

To reduce the impact of the thermal noise v , we perform an averaging of the estimated channel response over many DVB-T symbols. The static clutter suppression is performed in the frequency domain as follows:

$$X_f(k) = X_p(k) - \hat{H}_p(k)c_p(k) \quad \text{with } k = 1, \dots, K_p \quad (17)$$

Then, an inverse fast fourier transform (IFFT) is applied to obtain the time-domain filtered signal $x_f(n)$ which we can express as follows:

$$\begin{cases} H_0: x_f(n) = w(n), \\ H_1: x_f(n) = \alpha p(n - \kappa) e^{j2\pi f_d n} + w(n), \end{cases} \quad (18)$$

The noise $w(n)$ gathers the IFFT of V_p and the residual static clutter. Considering an efficient static clutter suppression, the variance of $w(n)$ can be approximated as follows:

$$\sigma_w^2 \simeq \frac{\sigma_v^2}{1 + \rho}, \quad (19)$$

3.3 Detection probability analysis

To evaluate the proposed detection strategy, we propose to analyse the detection probability behaviour. In order to do so, we need to calculate the statistics (mean and variance) of the cross-correlation (CC) detector output. The CC detection is performed by considering several values of time-delay and frequency-shifted copies of the reference signal and the surveillance signal. In our case, the reference signal is replaced by the generated pilot signal $p(n)$. The detection test is calculated as follows [20]:

$$T = |\bar{T}|^2 = \left| \sum_{n=0}^{N-1} T(n) \right|^2 \underset{H_0}{\overset{H_1}{\gtrless}} \lambda, \quad (20)$$

where the detection statistic is noted by \bar{T} and the detection threshold is λ .

The detection test is performed over all the considered range–Doppler cells. Here, we assume that the detection test is executed at the target cell (κ, f_d) . It follows that the generated pilot signal is time-delayed by κ and frequency-shifted by f_d to match with the target echo. The instantaneous output of the CC detector is given by

$$T(n) = x_f^*(n)p(n-\kappa)e^{-j2\pi f_d n}, \quad (21)$$

under the alternative hypothesis (H_1), we can calculate $T(n)$ as

$$T(n) = \alpha^* \left| p(n-\kappa) \right|^2 + w_p^*(n)p(n-\kappa)e^{-j2\pi f_d n}. \quad (22)$$

The mean value (under H_1) of the CC detector output, $T(n)$, is given by

$$E[T(n)|H_1] = \alpha^* \sigma_p^2, \quad (23)$$

and its variance can be expressed as follows:

$$\text{var}[T(n)|H_1] = |\alpha|^2 \sigma_p^4 + \sigma_w^2 \sigma_p^2, \quad (24)$$

by considering (19), we obtain

$$\text{var}[T(n)|H_1] = |\alpha|^2 \sigma_p^4 + \frac{\sigma_w^2 \sigma_p^2}{1 + \rho}. \quad (25)$$

To obtain the mean value and the variance of $T(n)$ under the null hypothesis (H_0), we set the parameter α to zero in (23) and (25), respectively.

The detection statistic \bar{T} results from a coherent integration of the CC detector output over N time samples. This can be expressed as

$$\bar{T} = \sum_{n=0}^{N-1} T(n). \quad (26)$$

If we consider the $T(n)$ samples as independent and identically distributed, the static \bar{T} (which is the sum of these samples) follows a complex Gaussian distribution under both hypotheses H_0 and H_1 [20]. The parameters (mean and variance) of the considered distribution can be obtained based on the parameters of $T(n)$ as follows:

$$\mu_0 = 0, \quad (27)$$

$$\sigma_0^2 = N \left(\frac{\sigma_w^2 \sigma_p^2}{1 + \rho} \right), \quad (28)$$

$$\mu_1 = N(\alpha^* \sigma_p^2), \quad (29)$$

$$\sigma_1^2 = N \left(|\alpha|^2 \sigma_p^4 + \frac{\sigma_w^2 \sigma_p^2}{1 + \rho} \right). \quad (30)$$

where (μ_0, σ_0^2) and (μ_1, σ_1^2) are the mean and variance of \bar{T} under H_0 and H_1 , respectively.

The false-alarm probability P_{FA} is calculated as follows [20]:

$$P_{FA} = \exp(-\lambda/\sigma_0^2), \quad (31)$$

and the detection probability for a given P_{FA} is obtained by

$$P_D = Q_1 \left(\sqrt{\frac{2|\mu_1|^2}{\sigma_1^2}}, \sqrt{\frac{2\sigma_0^2 \log(P_{FA}^{-1})}{\sigma_1^2}} \right). \quad (32)$$

To evaluate the capabilities of the proposed signal processing method, we calculate the resulting detection probability for different SNR values. Two SNR parameters are considered: the one of the reference signal SNR_r and that of the surveillance signal SNR. The retrieved results are compared to those of the conventional processing method [20] (needing a reference signal) and presented in Figs. 7 and 8. For both results, we considered a coherent processing interval of $N = 10^6$ samples and a false-alarm probability of 10^{-4} .

In Fig. 7, we notice the impact of the reference signal quality on the detection probability values. For high SNR_r values ($\text{SNR}_r > 10$ dB), the CC detector behaviour is similar to that of a matched filter and the detection probability is invariant for a given SNR value of the target. However, for low SNR_r values, the detection probability decreases for the same target SNR value by the degradation of the SNR_r value.

In Fig. 8, we present the detection probability results when a pilot signal replaces the reference signal for detection. Since no reference signal is used, the detection probability value depends only on the target SNR. As a result, we obtained a matched filter like results when the proposed method is applied. Consequently, the achieved performances (in terms of detection probability) of the

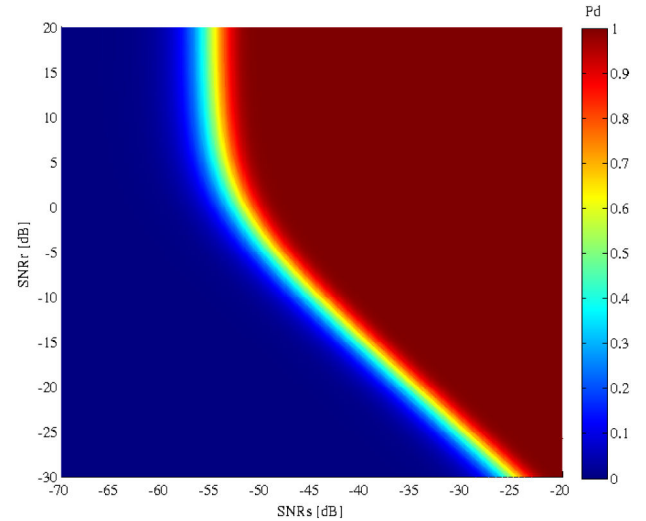


Fig. 7 Detection probability for the conventional CC detection as a function of the signals SNR for $N = 10^6$ and $P_{FA} = 10^{-4}$

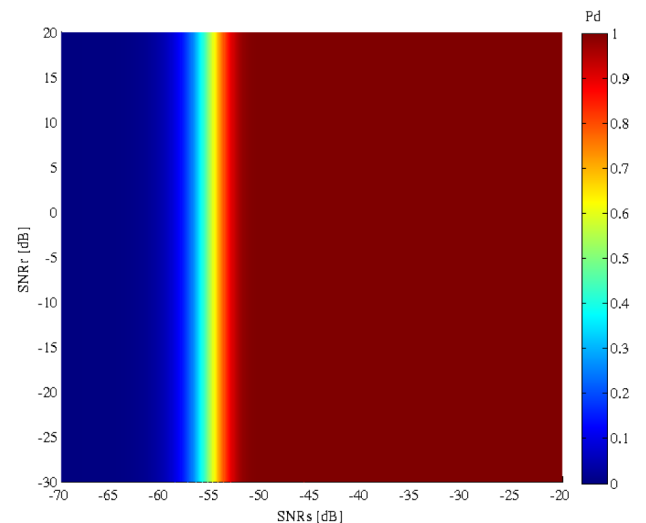


Fig. 8 Detection probability for the proposed CC detection as a function of the signals SNR for $N = 10^6$ and $P_{FA} = 10^{-4}$



Fig. 9 Setup employed for signal recording

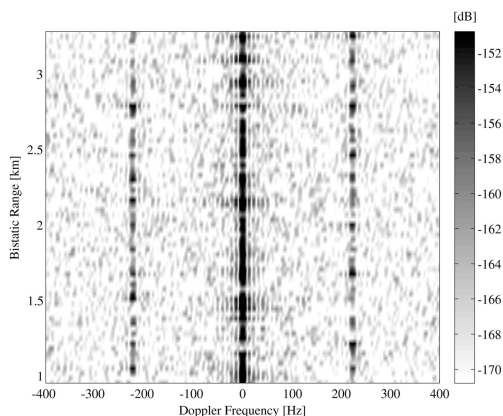


Fig. 10 Real-data result a range–Doppler diagram obtained using a pilot signal, a non-filtered received signal and a coherent integration interval of duration $T = 0.1$ s

proposed method are better than those for the conventional CC detection for low SNR_r values and the same for high SNR_r values.

4 Real-data results

To validate the theoretical retrievals, we apply the proposed detection strategy on real-data signals. The signals employed in this section have been recorded during a measurement campaign which was performed in Brussels at the Royal Military Academy (RMA). A proximate airport (Zaventem), located at 10 km from the receiver, offers the possibility of having echoes from low-altitude airplanes.

Fig. 9 shows the setup used for signal recording. The recording set-up includes a commercial Yagi antenna (MXR0012) with a gain of about 13 dBi, a USRP B100 device and a computer using the GNU radio software. The considered DVB-T transmitter is located at about 2.5 km from the receiver site and transmits at a frequency of 482 MHz with a radiated power of 10 kW. The DVB-T transmitters constellation operates in single frequency network mode.

Fig. 10 presents a range–Doppler diagram of a recorded signal. In this case, the received signal did not undergo the static clutter suppression stage. Consequently, we can notice the presence of the

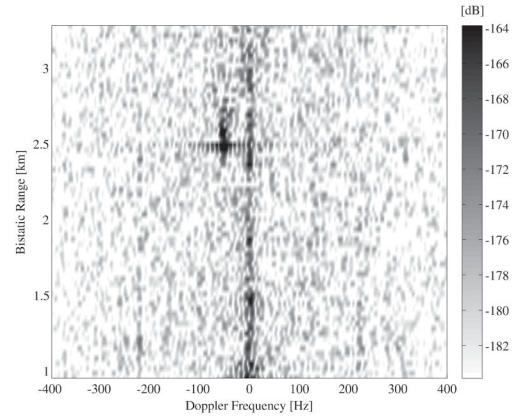


Fig. 11 Real-data result a range–Doppler diagram obtained using a full signal, a filtered received signal (ECA-C) and a coherent integration interval of duration $T = 0.1$ s

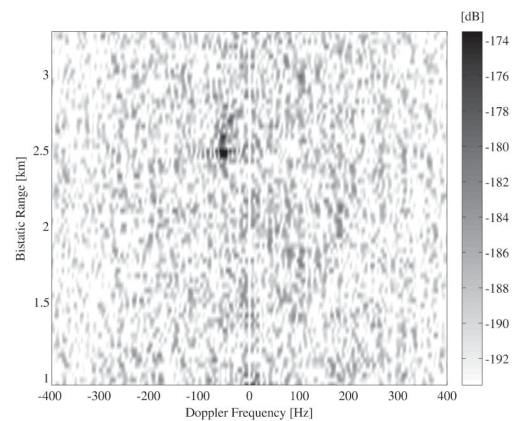


Fig. 12 Real-data result a range–Doppler diagram obtained using a full signal, a filtered received signal (the proposed method) and a coherent integration interval of duration $T = 0.1$ s

static clutter at 0 Hz. This undesirable component is masking a target echo which can be distinguished if the static clutter is removed.

Figs. 11 and 12 show the resulting range–Doppler diagrams after performing the ECA-C static clutter suppression method and the proposed method, respectively. For both diagrams, we can distinguish one target echo located at (2.5 km, -50 Hz). However, the proposed method enables an efficient suppression of the static clutter, in contrast with the ECA-C method where we can remark a considerable level of the residual static clutter. This validates the retrieved simulation results and demonstrates the feasibility of the proposed method in practice.

5 Conclusion

In this paper, we proposed an efficient signal processing method for PCL radars employing DVB-T signals. In this method, the reference signal is replaced by a locally-generated pilot signal and thus, no reference signal is required. This method reduces the cost and the complexity of the PCL system by using a signal reception channel. The proposed method includes an efficient static clutter suppression method based on the propagation channel estimation. The simulation results showed that using a pilot signal for detection outperforms the use of a received reference signal in low SNR scenarios, and it has the same performances for high SNR values. The real-data results validated the simulation results and proved the feasibility of the proposed method.

6 References

- [1] Willis, N.J.: ‘Bistatic radar’ (SciTech Pub, Raleigh, NC, USA, 2005)
- [2] Griffiths, H.D., Long, N.R.W.: ‘Television-based bistatic radar’, *IEE Proc. F, Commun. Radar Signal Process.*, 1986, **133**, (7), pp. 649–657

- [3] Cherniakov, M., Moccia, A.: 'Bistatic radar: emerging technology' (John Wiley & Sons, Chichester, UK, 2008)
- [4] Griffiths, H.D.D., Baker, C.J.J.: 'Passive coherent location radar systems. Part 1: performance prediction', *IEE Proc. Radar Sonar Navig.*, 2005, **152**, (3), p. 153
- [5] Baker, C.J.J., Griffiths, H.D.D., Papoutsis, I.: 'Passive coherent location radar systems. Part 2: waveform properties', *IEE Proc. Radar Sonar Navig.*, 2005, **152**, (3), p. 160
- [6] Howland, P.E., Maksimiuk, D., Reitsma, G.: 'FM radio based bistatic radar', *IEE Proc. Radar Sonar Navig.*, 2005, **152**, (3), p. 107
- [7] Malanowski, M., Kulpa, K., Kulpa, J., *et al.*: 'Analysis of detection range of FM-based passive radar', *IET Radar Sonar Navig.*, 2014, **8**, (2), pp. 153–159
- [8] Kubica, M., Kubica, V., Neyt, X., *et al.*: 'Optimum target detection using illuminators of opportunity'. 2006 IEEE Conf. on Radar, Verona, NY, USA, 2006, p. 8
- [9] Neyt, X., Raout, J., Kubica, M., *et al.*: 'Feasibility of STAP for passive GSM-based radar'. 2006 IEEE Conf. on Radar, Verona, NY, USA, 2006, p. 6
- [10] O'Hagan, D.W., Kuschel, H., Heckenbach, J., *et al.*: 'Signal reconstruction as an effective means of detecting targets in a DAB-based PBR'. 11-th Int. Radar Symp., Vilnius, Lithuania, 2010, pp. 1–4
- [11] Daun, M., Nickel, U., Koch, W.: 'Tracking in multistatic passive radar systems using DAB/DVB-T illumination', *Signal Process.*, 2012, **92**, (6), pp. 1365–1386
- [12] Berger, C.R., Demissie, B., Heckenbach, J., *et al.*: 'Signal processing for passive radar using OFDM waveforms', *IEEE J. Sel. Top. Signal. Process.*, 2010, **4**, (1), pp. 226–238
- [13] Palmer, J.E., Harms, H.A., Searle, S.J., *et al.*: 'DVB-T passive radar signal processing', *IEEE Trans. Signal Process.*, 2013, **61**, (8), pp. 2116–2126
- [14] Colone, F., O'Hagan, D.W., Lombardo, P., *et al.*: 'A multistage processing algorithm for disturbance removal and target detection in passive bistatic radar', *IEEE Trans. Aerosp. Electron. Syst.*, 2009, **45**, (2), pp. 698–722
- [15] Schwark, C., Cristallini, D.: 'Advanced multipath clutter cancellation in OFDM-based passive radar systems'. 2016 IEEE Radar Conf. (RadarConf), Philadelphia, PA, USA, 2016, pp. 1–4
- [16] Mahfoudia, O., Horlin, F., Neyt, X.: 'On the static clutter suppression for DVB-T based passive radars'. 32nd URSI General Assembly and Scientific Symp., Montreal, Canada, 2017
- [17] Cui, G., Liu, J., Li, H., *et al.*: 'Target detection for passive radar with noisy reference channel'. 2014 IEEE Radar Conf., Cincinnati, OH, USA, 2014, pp. 144–148
- [18] Cui, G., Liu, J., Li, H., *et al.*: 'Signal detection with noisy reference for passive sensing', *Signal Process.*, 2015, **108**, pp. 389–399
- [19] Baćzyk, M.K., Kulpa, K., Samczyński, P., *et al.*: 'The impact of reference channel SNR on targets detection by passive radars using DVB-T signals'. 2015 IEEE Radar Conf. (RadarCon), Arlington, VA, USA, 2015, pp. 708–712
- [20] Liu, J., Li, H., Himed, B.: 'On the performance of the cross-correlation detector for passive radar applications', *Signal Process.*, 2015, **113**, pp. 32–37
- [21] Baćzyk, M.K., Malanowski, M.: 'Decoding and reconstruction of reference DVBT signal in passive radar systems'. 2010 11th Int. Radar Symp. (IRS), Vilnius, Lithuania, 2010, pp. 1–4
- [22] Searle, S., Howard, S., Palmer, J.: 'Remodulation of DVB-T signals for use in passive bistatic radar'. 2010 Conf. Record of the Forty Fourth Asilomar Conf. on Signals, Systems and Computers (ASILOMAR), Pacific Grove, CA, USA, 2010, pp. 1112–1116
- [23] Mahfoudia, O., Horlin, F., Neyt, X.: 'Optimum reference signal reconstruction for DVB-T based passive radars'. 2017 IEEE Radar Conf. (RadarConf), Seattle, WA, USA, 2017
- [24] Mahfoudia, O., Horlin, F., Neyt, X.: 'Performance analysis of the reference signal reconstruction for dvb-t passive radars', *Signal Process.*, 2019, **158**, pp. 26–35
- [25] Chen, H.S., Gao, W., Daut, D.G.: 'Spectrum sensing for OFDM systems employing pilot tones and application to DVB-T OFDM'. 2008 IEEE Int. Conf. on Communications, Beijing, China, 2008, pp. 3421–3426
- [26] Danev, D., Axell, E., Larsson, E.G.: 'Spectrum sensing methods for detection of DVB-T signals in AWGN and fading channels'. 21st Annual IEEE Int. Symp. on Personal, Indoor and Mobile Radio Communications, Istanbul, Turkey, 2010, pp. 2721–2726
- [27] EBU/ETSI JTC: 'Digital video broadcasting (DVB); framing structure, channel coding and modulation for digital terrestrial television', Standaard, 2004
- [28] Mahfoudia, O., Horlin, F., Neyt, X.: 'Target detection for DVB-T based passive radars using pilot subcarrier signal'. 37th WIC Symp. on Information Theory in the Benelux, Louvain-la-Neuve, Belgium, 2016
- [29] Chabriel, G., Barrere, J., Gassier, G., *et al.*: 'Passive covert radars using CP-OFDM signals. A new efficient method to extract targets echoes'. 2014 Int. Radar Conf., Lille, France, 2014, pp. 1–6
- [30] Ochiai, H., Imai, H.: 'On the distribution of the peak-to-average power ratio in OFDM signals', *IEEE Trans. Commun.*, 2001, **49**, (2), pp. 282–289
- [31] Saini, R., Cherniakov, M.: 'DTV signal ambiguity function analysis for radar application', *IEE Proc. Radar Sonar Navig.*, 2005, **152**, (3), p. 133
- [32] Fechtel, S.A.: 'OFDM carrier and sampling frequency synchronization and its performance on stationary and mobile channels', *IEEE Trans. Consum. Electron.*, 2000, **46**, (3), pp. 438–441
- [33] Chen, S.-H., He, W.-H., Chen, H.-S., *et al.*: 'Mode detection, synchronization, and channel estimation for DVB-T OFDM receiver'. GLOBECOM '03. IEEE Global Telecommunications Conf. (IEEE Cat. No.03CH37489), San Francisco, CA, USA, 2003, vol. 5, pp. 2416–2420
- [34] van de Beek, J.J., Sandell, M., Borjesson, P.O.: 'ML estimation of time and frequency offset in OFDM systems', *IEEE Trans. Signal Process.*, 1997, **45**, (7), pp. 1800–1805
- [35] Liu, P., Li, B.-B., Lu, Z.-Y., *et al.*: 'A novel symbol synchronization scheme for OFDM'. Proc. 2005 Int. Conf. on Communications, Circuits and Systems, Hong Kong, China, 2005, vol. 1, pp. 247–251
- [36] Speth, M., Fechtel, S., Fock, G., *et al.*: 'Optimum receiver design for OFDM-based broadband transmission. II. A case study', *IEEE Trans. Commun.*, 2001, **49**, (4), pp. 571–578
- [37] Cardinali, R., Colone, F., Lombardo, P., *et al.*: 'Multipath cancellation on reference antenna for passive radar which exploits FM transmission'. IET Int. Conf. on Radar Systems, Edinburgh, UK, 2007, pp. 192–192
- [38] Wan, X., Cheng, F., Gong, Z., *et al.*: 'Multipath clutter rejection for digital radio mondiale-based HF passive bistatic radar with OFDM waveform', *IET Radar Sonar Navig.*, 2012, **6**, (9), pp. 867–872
- [39] van de Beek, J.J., Edfors, O., Sandell, M., *et al.*: 'On channel estimation in OFDM systems'. 1995 IEEE 45th Vehicular Technology Conf. Countdown to the Wireless Twenty-First Century, Chicago, IL, USA, 1995, vol. 2, pp. 815–819